Article

Supramolecular Assembly of Poly(phenylene vinylene) with Crown Ether Substituents To Form Nanoribbons

Yan-Hong Luo, Hong-Wei Liu, Fu Xi, Lin Li, Xi-Gao Jin, Charles C. Han, and Chi-Ming Chan

J. Am. Chem. Soc., **2003**, 125 (21), 6447-6451• DOI: 10.1021/ja0297739 • Publication Date (Web): 01 May 2003

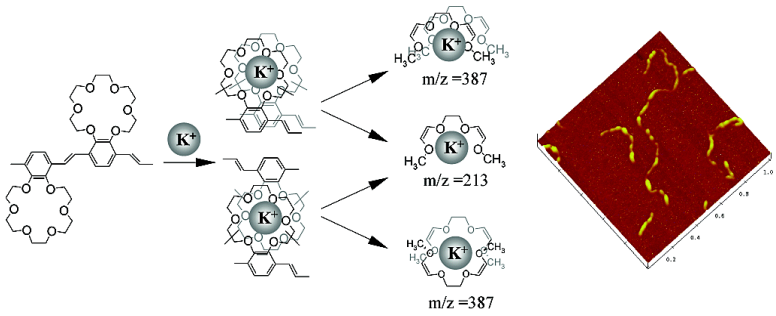

More About This Article

Additional resources and features associated with this article are available within the HTML version:

- Supporting Information
- Links to the 6 articles that cite this article, as of the time of this article download
- Access to high resolution figures
- Links to articles and content related to this article
- Copyright permission to reproduce figures and/or text from this article

View the Full Text HTML

J|A|C|S
ARTICLES
Published on Web 05/01/2003

Supramolecular Assembly of Poly(phenylene vinylene) with Crown Ether Substituents To Form Nanoribbons

Yan-Hong Luo,[†] Hong-Wei Liu,[†] Fu Xi,[†] Lin Li,*[,†] Xi-Gao Jin,[†] Charles C. Han,[†] and Chi-Ming Chan[‡]

Contribution from the Joint Laboratory of Polymer Science and Materials, State Key Laboratory of Polymer Physics and Chemistry, Institute of Chemistry, Chinese Academy of Sciences, Beijing 100080, China, and Department of Chemical Engineering, Hong Kong University of Science and Technology, Clear Water Bay, Hong Kong

Received December 17, 2002; E-mail: lilin@iccas.ac.cn

Abstract: Poly(*para*-phenylene vinylene) with crown ether substituents (C-PPV) could form nanoribbons through supramolecular assembly with K^+ in dilute chloroform solution. The length of the nanoribbons increased with an increase in the standing time of the C-PPV/K^+ solution. Experimental evidence to support the interaction between K^+ and crown ether substituents was provided, and the growth mechanism of C-PPV/K^+ nanorods to nanoribbons was proposed. The influence of the length of the nanoribbons on the photophysics of C-PPV was also investigated.

Introduction

Emissive conjugated polymers have attracted significant attention due to their electronic, optical, and energy-migration properties.[1−7] The preparation of well-defined nanostructures of a conjugated polymer, such as nanotubes and nanowires, is of considerable interest in the design of novel functional materials and nanoelectronic devices, such as nanosized transistors,[8,9] sensors,[10] etc.[2,11,12] Moreover, well-defined nanosized aggregates should be very useful for the understanding of the effects of interchain interactions on the emissive properties of conjugated polymers.[13,15,16] It is now generally accepted that interchain interactions play an important role in the luminescence processes of conjugated polymers.[14−21] Poly(*para*-phenylene vinylene) (PPV) and its derivatives are widely studied due to their superior photophysical properties.[15−17,22−25] Rothberg and co-workers estimated that up to 90% of the species formed upon excitation of poly(2-methoxy-5-(2′-ethylhexyloxy)-1,4-phenylene vinylene) (MEH-PPV) films are interchain.[17] Schwartz also found that the interchain species are aggregates with distinct ground-state absorption.[15,16] Studies of other polymers such as ladder-type poly(*para*-phenylene) and poly(*para*-pyridyl vinylene) show strong evidence for interchain aggregate formation in films.[18−21] However, the formation of interchain excited states in PPV and its derivatives is still a subject of much discussion.[15,16] Recently, we have reported on the synthesis of PPV samples with crown ether substituents (C-PPV).[25] It has been shown that potassium ions (K^+) induced the aggregation of C-PPV[25] and poly(*para* -phenylene ethynylene)s with 15-crown-5 substituents.[7] Here, we report on the formation of nanoribbons through the assembly of a conjugated polymer

[†] Chinese Academy of Sciences.
[‡] Hong Kong University of Science and Technology.

(1) Bernius, M. T.; Inbasekaran, M.; O'Brien, J.; Wu, W. S. *Adv. Mater.* **2000**, *12*, 1737.
(2) Hide, F.; Díaz-García, M. A.; Schwartz, B. J.; Andersson, M. R.; Pei, Q.; Heeger, A. J. *Science* **1996**, *273*, 1833.
(3) Friend, R. H.; Gymer, R. W.; Holmes, A. B.; Burroughes, J. H.; Marks, R. N.; Taliani, C.; Bradley, D. D. C.; Dos Santos, D. A.; Brédas, J. L.; Lögdlund, M.; Salaneck, W. R. *Nature* **1999**, *397*, 121.
(4) Kraft, A.; Grimsdale, A. C.; Holmes, A. B. *Angew. Chem., Int. Ed.* **1998**, *37*, 402.
(5) Levitsky, I. A.; Kim, J.; Swager, T. M. *J. Am. Chem. Soc.* **1999**, *121*, 1466.
(6) Kim, J.; McHugh, S. K.; Swager, T. M. *Macromolecules* **1999**, *32*, 1500.
(7) Kim, J.; McQuade, D. T.; McHugh, S. K.; Swager, T. M. *Angew. Chem., Int. Ed.* **2000**, *39*, 3868.
(8) Duan, X.; Huang, Y.; Cui, Y.; Wang, J.; Lieber, C. M. *Nature* **2001**, *409*, 66.
(9) Street, R. A.; Salleo, A. *Appl. Phys. Lett.* **2002**, *81*, 2887.
(10) Kong, J.; Franklin, N. R.; Zhou, C.; Chapline, M. G.; Peng, S.; Cho, K.; Dai, H. *Science* **2000**, *287*, 622.
(11) Gong, X.; Robinson, M. R.; Ostrowski, J. C.; Moses, D.; Bazan, G. C.; Heeger, A. J. *Adv. Mater.* **2002**, *14*, 581.
(12) An, K. H.; Kim, W. S.; Park, Y. S.; Choi, Y. C.; Lee, S. M.; Chung, D. C.; Bae, D. J.; Lim, S. C.; Lee, Y. H. *Adv. Mater.* **2001**, *13*, 497.
(13) Jenekhe, S. A.; Chen, X. L. *Science* **1998**, *279*, 1903.
(14) Jenekhe, S. A.; Osaheni, J. A. *Science* **1994**, *265*, 765.
(15) Nguyen, T. Q.; Doan, V.; Schwartz, B. J. *J. Chem. Phys.* **1999**, *110*, 4068.
(16) Nguyen, T. Q.; Martini, I. B.; Liu, J.; Schwartz, B. J. *J. Phys. Chem. B* **2000**, *104*, 237.
(17) Yan, M.; Rothberg, L. J.; Papadimitrakopoulos, F.; Galvin, M. E.; Miller, T. M. *Phys. Rev. Lett.* **1994**, *72*, 1104.
(18) Lemmer, U.; Heun, S.; Mahrt, R. F.; Scherf, U.; Hopmeier, M.; Siegner, U.; Göbel, E. O.; Müllen, K.; Bässler, H. *Chem. Phys. Lett.* **1995**, *240*, 373.
(19) Mahrt, R. F.; Pauck, T.; Lemmer, U.; Siegner, U.; Hopmeier, M.; Hennig, R.; Bässler, H.; Göbel, E. O.; Bolivar, P. H.; Wegmann, G.; Kurz, H.; Scherf, U.; Müllen, K. *Phys. Rev. B* **1996**, *54*, 1759.
(20) Blatchford, J. W.; Gustafson, T. L.; Epstein, A. J.; Vanden Bout, D. A.; Kerimo, J.; Higgins, D. A.; Barbara, P. F.; Fu, D. K.; Swager, T. M.; MacDiarmid, A. G. *Phys. Rev. B* **1996**, *54*, R3683.
(21) Blatchford, J. W.; Jessen, S. W.; Lin, L. B.; Gustafson, T. L.; Fu, D. K.; Wang, H. L.; Swager, T. M.; MacDiarmid, A. G.; Epstein, A. J. *Phys. Rev. B* **1996**, *54*, 9180.
(22) Pei, J.; Yu, W.; Huang, W.; Heeger, A. J. *Chem. Lett.* **1999**, 1123.
(23) Hsieh, B. R.; Yu, Y.; Forsythe, E. W.; Schaaf, G. M.; Feld, W. A. *J. Am. Chem. Soc.* **1998**, *120*, 231.
(24) Kim, K.; Jin, J. *Nano Lett.* **2001**, *1*, 631.
(25) Liu, H. W.; Wang, S.; Luo, Y. H.; Tang, W. H.; Yu, G.; Li, L.; Chen, C. F.; Liu, Y. Q.; Xi, F. *J. Mater. Chem.* **2001**, *11*, 3063.

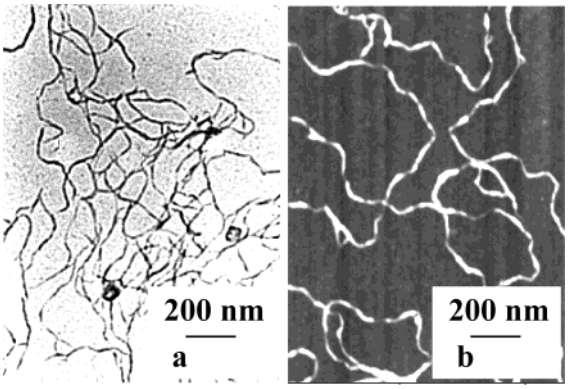

Figure 1. C-PPV/K^+ nanoribbons: (a) TEM image, (b) AFM height image. The height range of the image is 15 nm.

induced by K^+ in a chloroform solution and propose the formation mechanism for the nanoribbons. We also investigate the effects of the length of the nanoribbons on their photophysical properties.

Experimental Section

C-PPV was synthesized as described previously. The average molecular weight was measured to be 8.69×10^4 g/mol by laser light scattering.[25] C-PPV nanoribbons were prepared by adding a solution of KPF_6 in acetonitrile (2×10^{-2} M) to a solution of C-PPV in chloroform. The concentration of C-PPV ranged from 5×10^{-5} to 2×10^{-3} M. Samples of the nanoribbons for the atomic force microscopy (AFM) study were prepared by spin-coating the C-PPV/K^+ solution on silicon wafers. AFM images were recorded under ambient conditions using a Digital Instrument Multimode Nanoscope IIIA operating in the tapping mode. Si cantilever tips (TESP) with a resonance frequency of approximately 300 kHz and a spring constant of about 40 Nm^{-1} were used. The scan rate varied from 0.5 to 1.5 Hz. The set-point amplitude ratio ($r_{sp} = A_{sp}/A_o$, where A_{sp} is the set-point amplitude, and A_o is the amplitude of the free oscillation) was adjusted to 0.7−0.9. All AFM images shown here were subjected to a first-order plane-fitting procedure to compensate for sample tilt. Transmission electron microscopy (TEM) measurements were performed on a Hitachi H-800 electron microscope operated at 100 kV. Samples of nanoribbons for the TEM study were prepared by casting the C-PPV/K^+ solution onto carbon-coated copper grids.

Time-of-flight secondary ion mass spectrometry (ToF−SIMS) measurements were performed on a Physical Electronics PHI 7200 TOF−SIMS spectrometer. The primary ions were generated from a Cs ion source (8 kV). The total ion dose for each spectrum acquisition was $<4 \times 10^{11}$ ions/cm^2. Both positive and negative high-resolution mass spectra were recorded.

Absorption and photoluminescence spectra were obtained using a General TU-1201 UV recording spectrophotometer and a Hitachi F-4500 fluorescence spectrophotometer, respectively.

Results and Discussion

Figure 1a and b shows a TEM micrograph and an AFM height image of the nanoribbons, respectively. The standing time for both samples was 70 days. The C-PPV concentration was 5×10^{-5} M, and the mole ratio of crown ether to potassium ion was 1:6. Nanoribbons, with an average width of 15 nm measured from the TEM micrograph, can be clearly observed. The widths of the nanoribbons can be measured using TEM and AFM. However, the widths of nanoribbons measured by TEM are smaller than those measured by AFM due to the broadening

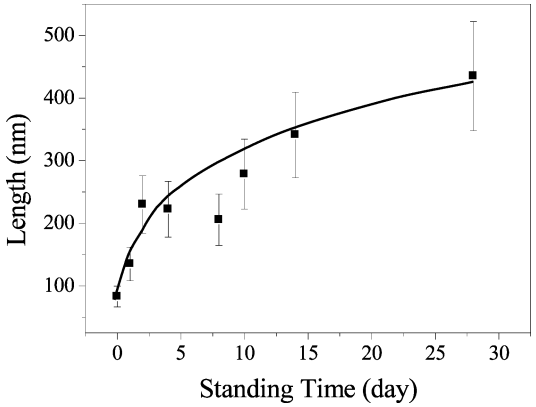

Figure 2. The average length of the nanoribbons versus the standing time of a C-PPV/K^+ solution in the presence of K^+. The average length was measured by AFM.

effects of AFM measurements.[26,27] The thickness of the nanoribbons which cannot be measured from the TEM micrographs was measured through the cross-section analysis of the AFM height images.

After the addition of K^+ to the solution of C-PPV, no precipitation was seen, and the solution was stable for an extended period of time. Figure 2 shows that the average length of nanoribbons without branches, measured by AFM, increased with time. Nanorods were first observed about 30 min after the addition of K^+ in a 5×10^{-5} M C-PPV solution. The average length of the nanorods was less than 100 nm (cf., Figures 2 and 3a). When the solution was kept under ambient conditions for 20 days, the average length of the nanoribbons increased to above 400 nm. Seventy days after the addition of K^+ in the solution, most of the strands had lengths over several micrometers, as shown in Figure 1.

Figure 3b and c shows the height images of the nanoribbons after 70 days. Through the cross-section analysis of the height images, the average thickness of these nanoribbons was measured to be about 3 nm. The nanorods joined together at their ends forming nanoribbons with or without branches, as labeled with B in Figure 3b. The nanorods might also join together at their ends forming nanoribbon rings (labeled with R), as shown in Figure 3c. Figure 3d shows the cross-section profile of line d in Figure 3b. It was found that the thickness at the joints of the ends of two nanorods was about 1−2 nm less than the average thickness of the nanoribbons (cf., P in Figure 3d). In addition to the joints of their ends, the nanoribbons might overlap with each other to form a crossing site, labeled with O and O1 in Figure 3b and c, respectively. The crossing and branching sites can be distinguished by the AFM cross-section analysis. The AFM cross-section profiles of lines d and e in Figure 3b and line f in Figure 3c were shown in Figure 3d, e, and f, respectively. It is clearly demonstrated that the thickness of the crossing sites was almost twice the average thickness of the nanoribbons. The joining of the nanorods and the crossing of the nanoribbons lead to the observation of branches and rings, as shown in Figure 3b and c. Moreover, only dots with diameters above 20 nm were seen on the sample prepared by spin-casting the same C-PPV solution without potassium ions on a silicon

(26) Bustamante, C.; Keller, D. *Phys. Today* **1995**, *48*, 32.
(27) Samorí, P.; Francke, V.; Müllen, K.; Rabe, J. P. *Chem.-Eur. J.* **1999**, *5*, 2312.

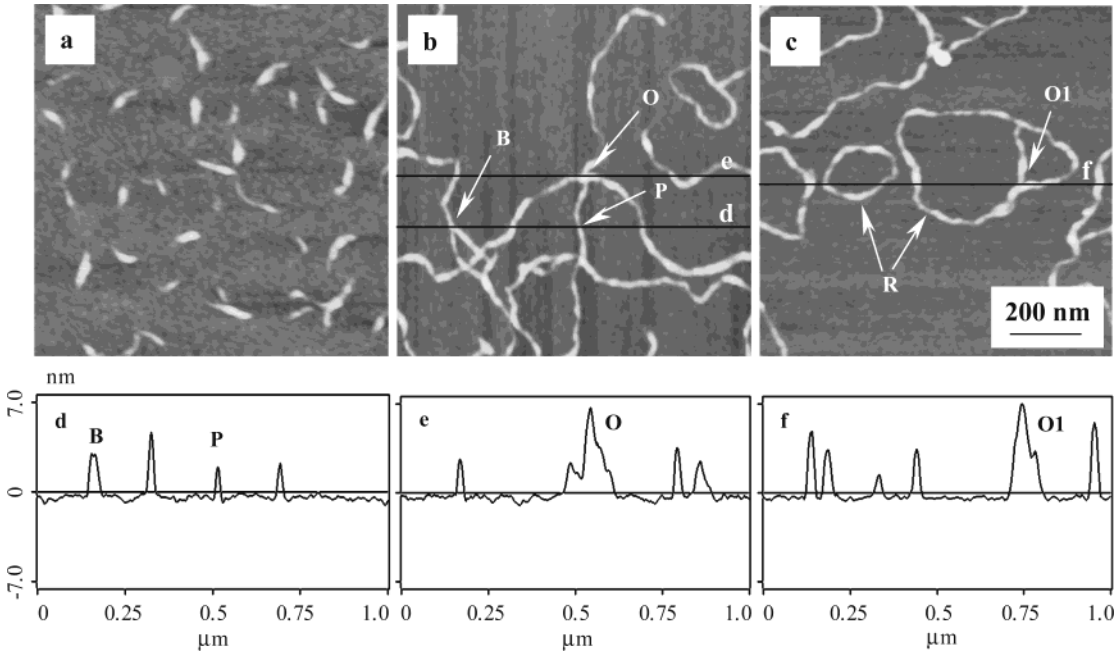

Figure 3. AFM images of (a) nanorods formed 30 min after the addition of K^+, (b) and (c) nanoribbons formed 70 days after the addition of K^+. (d−f) AFM cross-section profiles. The height range of the AFM images is 15 nm.

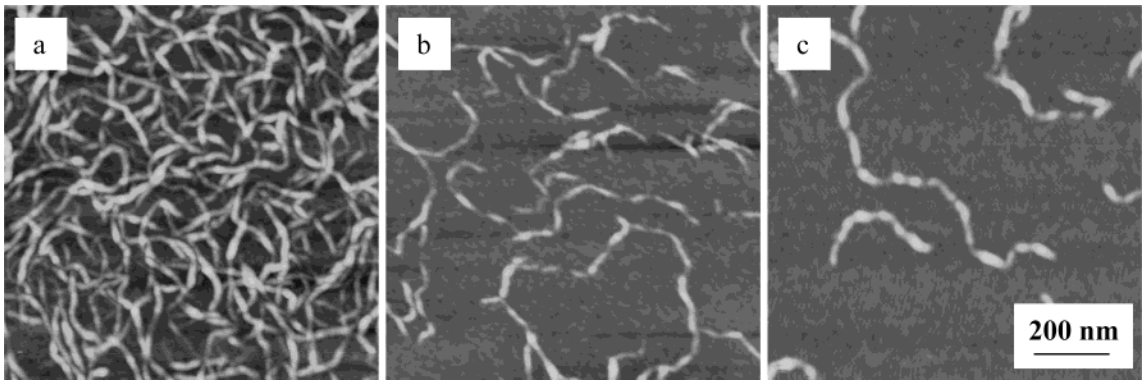

Figure 4. AFM images of (a) a nanoribbon net formed using a 4×10^{-4} M C-PPV solution after the addition of K^+ for 30 min, (b) and (c) nanoribbons after the solution of (a) was diluted to 1×10^{-4} and 5×10^{-5} M, respectively. The height range of the images is 15 nm.

wafer.[25] It is clear that nanoribbons with an average width of about 15 nm, an average thickness of about 3 nm, and lengths over several micrometers were produced via the assembly of C-PPV induced by K^+ in solution.

As we have investigated, the longer the standing time of a C-PPV/K^+ solution, the longer the nanoribbons will grow, and the more branches and nanoribbon rings were observed. The morphology of the nanoribbons was found to be independent of the C-PPV concentration in the range from 5×10^{-5} to 2×10^{-3} M. However, the amount and the average length of the nanoribbons increased significantly when a higher concentration of the C-PPV solution was used. A nanoribbon net was observed when spin-coating a 4×10^{-4} M C-PPV/K^+ solution (after the solution was standing at room temperature for 30 min after the addition of K^+, the mole ratio of crown ether to K^+ was 1:1) on a silicon wafer, as shown in Figure 4a. After the C-PPV/K^+ solution was diluted, the nanoribbon net was dissociated, leading to the observation of nanoribbons, as shown in Figure 4b (1×10^{-4} M) and c (5×10^{-5} M).

When the concentration of the C-PPV/K^+ solution was above 4×10^{-4} M, precipitation occurred after a long standing time. These results also confirm that the formation of the C-PPV nanoribbons is induced by K^+ and occurs in the bulk solution rather than during the spin-coating process.

It has been postulated that the formation of the 2:1 sandwich complex between K^+ ions and crown ether substituents brings two polymer chains closer together.[7] The K^+ ions create interpolymer bridges and induce the formation of the C-PPV aggregates in the solution, as illustrated in Scheme 1. In addition, the attractive $\pi-\pi$ interactions among the aromatic rings also promote the formation of the aggregates. To maintain electroneutrality, the counteranions (PF_6^-) must diffuse to the positively charged backbones. The accumulation of the negative counterions surrounding the aggregates produces an electrostatically shielded effect, preventing further aggregation of the nanorods except at their ends. The average contour length of the C-PPV chains was estimated to be about 200 nm, and the average length of the nanorods was less 100 nm. Therefore, we postulated that the K^+ ions first form bridges between some segments of the C-PPV chains with untrapped segments as protruding cilia at the two ends of the nanorods. When the solution is kept for an extended period of time, the free K^+ ions then forms bridges

Scheme 1. A Schematic Drawing of the C-PPV Aggregation Process Induced by K^+ in the Solution

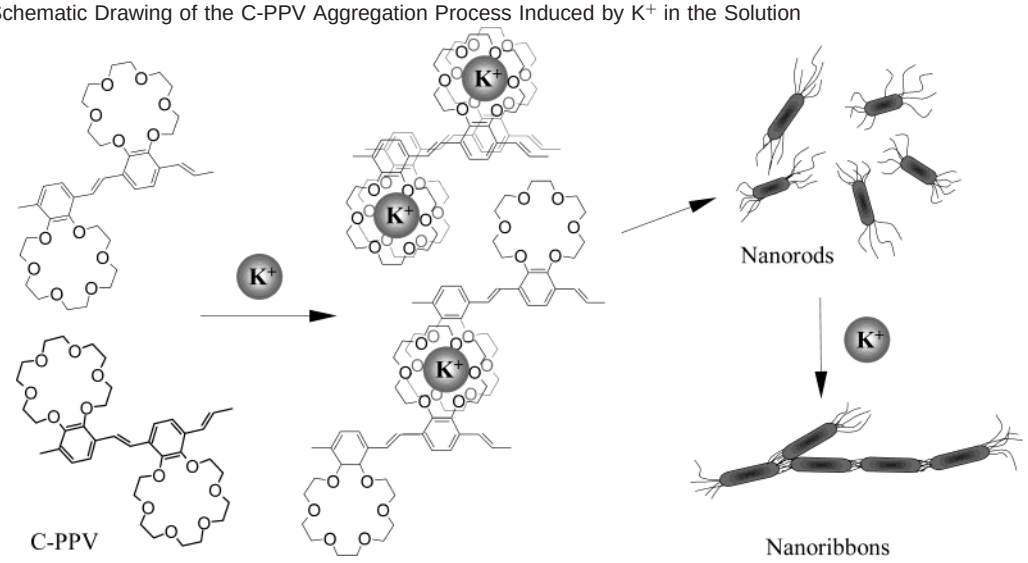

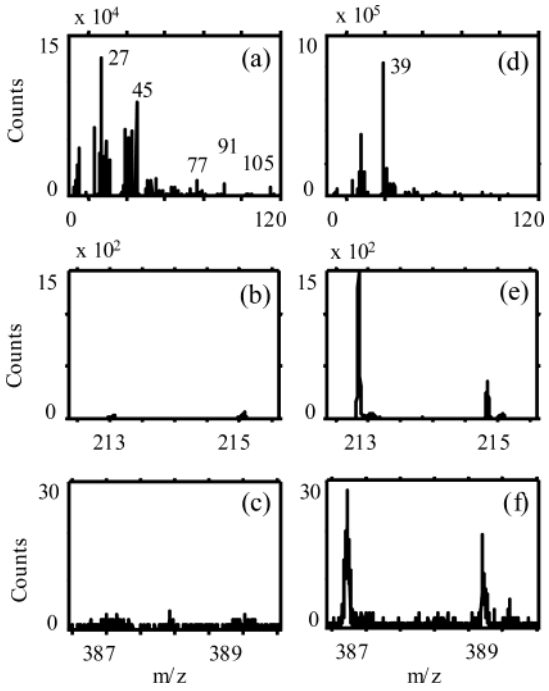

Figure 5. (a−c) and (d−f) are positive ToF−SIMS spectra of C-PPV and the C-PPV/K^+ nanoribbons, respectively.

between the protruding cilia of the nanorods, producing nanoribbons with and without branches. When the two ends of the nanoribbons join together, nanoribbon rings form (cf., Scheme 1 and Figure 3).

To provide additional support for the mechanism of the formation of K^+ ion interpolymer bridges, the mass spectra for C-PPV and the C-PPV/K^+ nanoribbons were obtained using ToF−SIMS. As shown in Figure 5, the fragments for linear and aromatic hydrocarbons, such as $m/z = 27$ ($C_2H_3^+$), 45 ($C_2H_5O^+$), 77 ($C_6H_5^+$), 91 ($C_7H_7^+$), and 105 ($C_8H_9^+$) amu, are dominant in the positive ToF−SIMS spectrum of C-PPV (cf., Figure 5a), and the $K^{(39)+}$ ion ($m/z = 39$ amu) is the most intense peak in the spectrum of C-PPV/K^+ nanoribbons (cf., Figure 5d). Two pairs of characteristic fragments [213 amu ($C_8H_{14}O_4K^{(39)+}$) and 215 amu ($C_8H_{14}O_4K^{(41)+}$), as well as 387 amu ($C_{16}H_{28}O_8K^{(39)+}$) and 389 amu ($C_{16}H_{28}O_8K^{(41)+}$)] are

Scheme 2. Fragmentation Pathways of the C-PPV/K^+ Nanoribbons To Show the Formation of K^+ Bridges

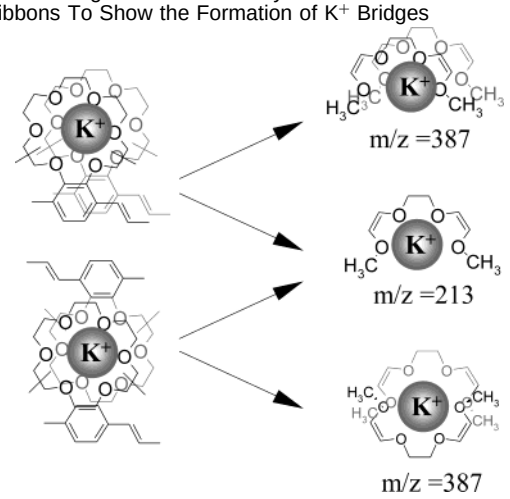

observed in the positive ToF−SIMS spectrum of the C-PPV/K^+ nanoribbons (cf., Figure 5e and f). The possible fragmentation pathways and the chemical structures of these fragments are shown in Scheme 2. The observation of the characteristic fragments ($C_8H_{14}O_4K^{(39)+}$ and $C_{16}H_{28}O_8K^{(39)+}$) only in the ToF−SIMS spectrum of the C-PPV/K^+ nanoribbons suggests that the formation of the 2:1 sandwich complexes between K^+ and the crown ether substituents because the recombination of ions seldom occurs during the ToF−SIMS process.[28,29]

The effects of interchain interactions of C-PPV in the nanoribbons on the photophysical properties were investigated using UV absorption (UV) and photoluminescence (PL) spectrophotometers. The UV and PL spectra are shown in Figure 6. Clearly, the UV spectra for the nanorods and nanoribbons exhibit substantial broadening and red shifts. The absorption maximum shifts from 442 nm for C-PPV to 461 nm for nanoribbons, and a shoulder absorption band appears at 490 nm. Similarly, the fluorescence spectrum for the nanoribbons quenches drastically (quenching about 97%) with a broad band centered at 531 nm.

(28) Chan, C. M. *Polymer Surface Modification and Characterization*; Hanser: New York, 1994.
(29) Zhou, H.; Chan, C. M.; Weng, L. T.; NG, K. M.; Li, L. *Surf. Interface Anal.* **2002**, *33*, 932.

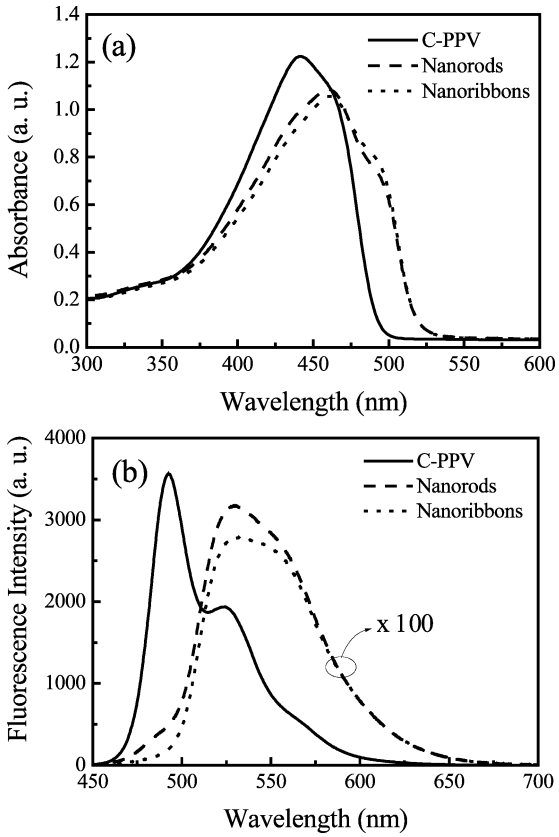

Figure 6. (a) UV absorption and (b) PL emission spectra of C-PPV chloroform solution in the absence of and presence of K^+. The concentration of C-PPV is 5×10^{-5} M, and the PL excitation wavelength is 440 nm.

The complete disappearance of the peak at 490 nm, which corresponds to isolated polymer chains, indicates that most of the chain segments form aggregates. We also investigated the effects of the length of nanoribbons on the UV and PL properties. There are no apparent differences between the spectra of nanorods (~100 nm in length) and nanoribbons (~400 nm in length), as shown in Figure 6. These results indicate that the red shift of the C-PPV characteristic peaks does not change after the aggregates grow to a certain size.[14−17]

Conclusion

In summary, we report the formation of the C-PPV/K^+ nanorods and the growth of the nanorods to the nanoribbons. The growth mechanism of the nanorods to the nanoribbons was proposed. The K^+ ions first form bridges between some segments of the C-PPV chains with untrapped segments as the protruding cilia at the two ends of the nanorods. The formation of more bridges between the free K^+ ions and the protruding cilia of the nanorods leads to the connection of the nanorods at their ends, producing nanoribbons. The crossing of nanoribbons and the joining of nanorods can be analyzed and distinguished through the AFM height measurements. These lead to the current understanding of the formation of the nanoribbons with or without branches and rings (as shown in Scheme 1). The formation of the C-PPV/K^+ bridges was verified by ToF−SIMS analyses.

Acknowledgment. This project is supported by the National Science Foundation of China (Grant No. 50273044), the National Science Foundation of China, and the Hong Kong Government Research Grants Council Joint Research Scheme under Grant Nos. NSFC 20131160730 and N_HKUST 618/01.

JA0297739